frontiers | Frontiers in Energy Research

TYPE Original Research
PUBLISHED 17 October 2024
DOI 10.3389/fenrg.2024.1485470

OPEN ACCESS

EDITED BY
Vijay Kumar,
National Institute of Technology, Srinagar, India

REVIEWED BY
Akshit Samadhiya,
Sandip University, India
Nishant Thakkar,
Amrita Vishwa Vidyapeetham University, India
Jitendra Bahadur,
Amrita Vishwa Vidyapeetham University (Bangalore), India
Devakirubakaran S,
SRM Institute of Science and Technology, India

*CORRESPONDENCE
Ahmad Taher Azar,
aazar@psu.edu.sa
Ibrahim A. Hameed,
ibib@ntnu.no

RECEIVED 23 August 2024
ACCEPTED 04 October 2024
PUBLISHED 17 October 2024

CITATION
Torchani B, Azar AT, Sellami A, Ahmed S, Hameed IA, Kasim Ibraheem I and Al-Obaidi MIJ (2024) Adaptive sliding mode control based on maximum power point tracking for boost converter of photovoltaic system under reference voltage optimizer.
Front. Energy Res. 12:1485470.
doi: 10.3389/fenrg.2024.1485470

Adaptive sliding mode control based on maximum power point tracking for boost converter of photovoltaic system under reference voltage optimizer

Borhen Torchani[1], Ahmad Taher Azar[2,3,4]*, Anis Sellami[1], Saim Ahmed[2,3], Ibrahim A. Hameed[5]*, Ibraheem Kasim Ibraheem[6] and Moamin Ibrahim Jameel Al-Obaidi[7]

[1]LISIER Laboratory, ENSIT, University of Tunis, Tunis, Tunisia, [2]College of Computer and Information Sciences, Prince Sultan University, Riyadh, Saudi Arabia, [3]Automated Systems and Soft Computing Lab (ASSCL), Prince Sultan University, Riyadh, Saudi Arabia, [4]Faculty of Computers and Artificial Intelligence, Benha University, Benha, Egypt, [5]Department of ICT and Natural Sciences, Norwegian University of Science and Technology, Alesund, Norway, [6]Department of Electrical Engineering, College of Engineering, University of Baghdad, Baghdad, Iraq, [7]Department of Communication Technical Engineering, Uruk University, Baghdad, Iraq

This article presents an innovative APISMC method applied to PVS, integrating the MPPT technique for a boost converter. The primary objective of this approach is to maximize the converter's output power while ensuring optimal operation in the face of varying environmental conditions such as solar irradiance and temperature, while dynamically adapting to variations in system parameters, as demonstrated by the obtained results. To achieve this, a RVO is employed to generate reference voltage and power. A PI controller calculates the reference current based on this power. The APISMC control modeling utilizes all its reference variables to synthesize the sliding surface and duty cycle for optimal boost converter control. Simulations conducted demonstrate superior performance in terms of stability, speed, and control of the converter compared to traditional MPPT algorithms. The main contributions of this article include an improvement in system robustness against irradiance variations, thanks to the integration of an adaptive algorithm and a PI controller within the SMC. Moreover, the proposed theoretical and practical framework enables rapid MPPT attainment by adjusting the duty cycle in real-time, optimizing maximum power extraction and ensuring stable regulation even under non-ideal conditions.

KEYWORDS

photovoltaic system, boost converter, reference voltage optimizer, maximum power point tracking, adaptive sliding mode control

Abbreviations: PV, Photovoltaic; APISMC, Adaptive Proportional Integral Sliding Mode Control; PVS, Photovoltaic Systems; MPPT, Maximum Power Point Tracking; RVO, Reference Voltage Optimizer; SMC, Sliding Mode Control; PI, Proportional Integral; MPP, Maximum Power Point; PO, Perturbation and Observation.

1 Introduction

Renewable energies are alternative energy sources to fossil fuels, which are limited and polluting. They are essential for the energy transition towards a more sustainable world. Among renewable energies, PV solar energy is one of the most promising. It is clean, inexhaustible, and available in most countries around the world. It is rapidly developing and becoming increasingly efficient and affordable. However, the most important challenge is to find technical means to maximize the energy production of PVS, particularly through better control of converters. Thus, their performance heavily depends on the control techniques applied. One of the techniques often used and commercialized is MPPT. Indeed, it is an algorithm that allows for finding the MPP of a PV system. In other words, it can be characterized as the point where the output power generated by the converter system is maximized for a given output voltage. Several studies have focused on the control of PVS using the MPPT technique (Poongavanam et al., 2023; Velmurugan et al., 2022; Vankadara et al., 2022; Vankadara et al., 2023). Various types of classic MPPT algorithms have been developed for PVS, such as the Incremental Conductance (INC) algorithm, which offers good responsiveness to rapid changes but may suffer from increased complexity and sensitivity to measurement errors (Atia et al., 2022; Chellakhi et al., 2024; El Ouardi et al., 2023; Ahmed et al., 2022). The RVO control is another approach that adjusts the reference voltage to maximize power but may be limited by non-ideal operating conditions (El Fadili et al., 2014). Also noteworthy is the PO control, which is simple to implement and effective under steady-state operating conditions (Ali and Mohamed, 2022; Gomathi et al., 2024; Kumar and Bindal, 2022). However, it may perform less well under rapid variations in irradiation, leading to oscillations around the MPP, among other commonly used techniques. These techniques are straightforward to implement and provide good performance. Nevertheless, they can be sensitive to variations in temperature and illumination. Currently, new control techniques for PVS and converters are being developed, including those utilizing artificial intelligence (Remoaldo and Jesus, 2021; Mazumdar et al., 2024; Aljafari et al., 2023; Radhakrishnan et al., 2022; Oliver et al., 2022), such as neural networks control algorithm (Cano et al., 2024; Maguluri et al., 2023; Oh et al., 2024; Sahoo et al., 2022; Saxena et al., 2021), fuzzy logic control (Abdelmalek et al., 2018; Chandrashekar et al., 2024; Derbeli et al., 2023; Hussain et al., 2024), and adaptive controls (Henao-Bravo et al., 2022; Li et al., 2024; Stitou et al., 2022; Ouaret et al., 2023).

PVS are subjected to sudden external variations, such as changes in temperature and irradiation. However, traditional controllers are often ineffective and lack robustness against these external disturbances. Therefore, converters generally require high-performance and robust controls in terms of speed and accuracy to meet the load requirements under variable conditions and to maintain performance even in the presence of uncertainties and disturbances. In reality, PV systems, where the converter is a key element, require good regulation of their duty cycle (Corrêa and Vieira, 2023; Youssef et al., 2023). Maintaining precise duty cycle control is essential for optimizing the voltage and power at the output of the converter. For this reason, robust, adaptive, and fuzzy controls are more complex but offer better robustness against environmental variations. For this work, Sliding Mode Control (SMC) is recognized for its robustness and ability to manage nonlinear systems, making it a preferred choice for PVS (Chaibi et al., 2019; Muktiadji et al., 2022; Singh et al., 2017; Swarnkar et al., 2022). By its nature, this control is a nonlinear control algorithm that allows for managing the dynamic systems of the PV and the converter in the presence of disturbances and uncertainties (Azar and Serrano, 2015; Chang et al., 2024; Gundecha et al., 2016; Tian et al., 2019; Samadhiya et al., 2021; Samadhiya and Namrata, 2021; Vaidyanathan and Azar, 2016). It is based on constructing a sliding surface, which represents the operating space of these two systems. The SMC maintains the dynamical system on the sliding manifold modeled by the system's current and voltage relative to the reference currents and voltages. This ensures its correct operation and rapid response. The choice of parameters for the sliding surface is a crucial point for optimizing the control operation from a dynamic and rapid perspective. Thus, the combination of SMC control and adaptive parameter control leads to a certain optimization that enhances the performance of conventional SMC control to very significant results. Several studies have addressed the integration of SMC control with adaptive control (Alnami et al., 2024; Rahme et al., 2023), neural networks (Ruz-Hernandez et al., 2024; Wang et al., 2023), PI controllers (Bhat et al., 2020; Chinnappan et al., 2019), and fuzzy logic (Ezhilan et al., 2022; Said Adouairi et al., 2023).

In the literature cited in previous paragraphs, many existing MPPT techniques, such as Incremental Conductance and Perturbation and Observation, exhibit sensitivity to environmental variations, leading to degraded performance during rapid changes in irradiation or temperature, resulting in oscillations around the maximum power point. Additionally, traditional controllers often lack robustness against external disturbances, making it difficult to accurately regulate the output voltage and converter performance. Another noteworthy point is the complexity of algorithms. Indeed, several recent approaches, particularly those using artificial intelligence, while effective, can be too complex for practical and robust implementation in real-time systems. The APISMC proposed in this article aims to address these shortcomings by integrating an adaptive control that allows for dynamic adjustment of control parameters based on environmental variations, thus improving system stability and response speed. Additionally, APISMC control relies on robustness, combining SMC control with adaptive algorithms, the approach ensures accurate regulation of the output voltage, even in the presence of uncertainties and disturbances.

The article presents an innovative APISMC control method applied to PVS, integrating the MPPT technique for the boost converter. This approach aims to maximize the converter's output power while ensuring optimal operation, even in the face of environmental variations such as solar irradiance and temperature. Consequently, a new MPPT approach is designed, using APISMC control for the PVS and the boost converter, aimed at improving robustness against environmental variations and subsequently maximizing the extracted power. Furthermore, the improvement of robustness against irradiation variations is achieved by integrating the PI controller and the adaptive algorithm into the SMC control. Simulation results show that the APISMC MPPT algorithm offers superior performance compared to conventional MPPT algorithms under SMC or PO control. It is capable of quickly

tracking changes in irradiation and maintaining maximum output power by monitoring it against the reference. However, it should not be overlooked that traditional MPPT controllers, which are simple to implement and provide good performance under nominal conditions, can be sensitive to variations in temperature and irradiation.

The organization of this article is as follows: In Section 2, we will present the PV model by outlining the main mathematical equations relating the photo-generated current to solar irradiation and temperature, the total current, and finally the power provided by the panel. Afterwards, the modeling of the boost converter will be established in Section 3. The converter is presented through the relationships that connect the input and output voltages of the converter and the current through the coil, which is often confused with the output current. This modeling includes the integration of the duty cycle between the input and output electrical variables, leading to the development of the output power of the converter. The importance of the RVO technique and its operating algorithm are discussed in Section 4. In Section 5, we emphasize the objectives of the APISMC control and the benefits of integrating the adaptive algorithm and PI control into the SMC. The development of the suggested APISMC will be discussed in Section 6, involving the designing of the sliding surface and the various components of the proposed control system, and also the confirmation of the system's stability through the use of the APISMC. In Section 7, the application of the proposed control will be implemented through numerical simulations of the photovoltaic system and the boost converter. The effectiveness of the proposed control is verified against other control techniques. Finally, in Section 8, we will present a conclusion highlighting the main results obtained and potential perspectives to conclude this work.

2 Modeling of the photovoltaic system

In this section, we propose the modeling of a cell in a PVS. The various mathematical equations materializing this electrical diagram of the photovoltaic cell will be given below.

2.1 Equation of the PV module current

The equation for the current of the PV module is given as follows:

$$I_{pv} = I_{ph} - I_0\left(exp\left(V_{pv} + I_{pv}R_s \middle/ aN_sV_{th}\right) - 1\right) \quad (1)$$

The different variables and parameters of Equation 1 are given in nomenclatures section at the beginning.

2.2 Equation for the total current of the PV system

To obtain this equation, we divide the current of the PV module I_{pv} by the number of PV modules n_p connected in parallel.

$$I_{in} = \frac{I_{pv}}{n_p} \quad (2)$$

I_{in} Is the total current generated by the PV panel (A).

2.3 Equation of the photo-generated current

The photo-generated current depends on the illumination and the temperature:

$$I_{ph} = \left(I_{sc,n} + k_i \times (T - T_n)\right) \times \left(G/G_n\right) \quad (3)$$

where the different parameters of Equation 3 are defined in nomenclatures section at the beginning.

2.4 Power equation of the PVS

The electrical power generated by the PV panel is the product of the current given by Equation 2 and the voltage, and it is expressed as follows:

$$P_{in} = I_{in} \times V_{in} \quad (4)$$

the parameters of Equation 4 are given by:

P_{in} is the power generated by the PV panel (W)

V_{in} is the voltage generated by the PV panel (V)

3 The boost converter

To adapt the output voltage of the photovoltaic system to the load, we plan to choose a boost-type voltage converter. The focus will be on the equations relating the input and output voltage of the converter to the current flowing through the inductor circuit. In reality, the inductor current I_L is often confused with the output current of the converter noted I_{out}.

3.1 Presentation of the boost converter

The boost converter is governed by the two known operating modes called '*ON*' and '*OFF*'. The input voltage-output voltage relationship can be described as follows:

$$\begin{cases} L\dfrac{di_L}{dt} = V_{in} + (\mu - 1)V_{out} \\ C\dfrac{dV_{out}}{dt} = -i_{out} - (\mu - 1)i_L \end{cases} \quad (5)$$

with

i_L is the instantaneous current of the inductance passing through the coil in (A),

i_{out} is the instantaneous output current in (A),

V_{out} is the output voltage in (V), μ is a logical variable that can only take the values 0 or 1 depending on the operating state of the boost converter, such as:

$$\begin{cases} \mu = 0 & \text{switch } ON \\ \mu = 1 & \text{switch } OFF \end{cases}$$

The input voltage V_{in} and output voltage V_{out} can be expressed as:

$$V_{in} = \begin{cases} V_{out} + L\dfrac{di_L}{dt} & \text{if } \mu = 0 \\ L\dfrac{di_L}{dt} & \text{if } \mu = 1 \end{cases} \tag{6}$$

and

$$V_{out} = \begin{cases} -\dfrac{1}{C}\displaystyle\int (i_{out} + i_L)dt & \text{if } \mu = 0 \\ -\dfrac{1}{C}\displaystyle\int i_{out}dt & \text{if } \mu = 1 \end{cases} \tag{7}$$

Using Equations 4–7, we can reformulate this converter problem based on the dynamics control relying on the voltage V_{in}, voltage V_{out} and current I_L. Afterwards, we will present the sizing of voltages V_{in} and V_{out} as a function of the duty cycle D and then the output power for which we will perform the MPPT.

3.2 Duty cycle of the boost converter

The integration of D into the modeling of a photovoltaic system is crucial for optimizing power extraction and ensuring efficient operation of the converter. By adjusting D according to sunlight conditions and system characteristics, it is possible to enhance the overall performance of the PVS.

For a boost converter, the duty cycle D is defined by:

$$D = \frac{V_{out}}{V_{out} + V_{in}} \tag{8}$$

Equation 8 shows that the duty cycle is proportional to the output voltage relative to the sum of the input and output voltages. A higher duty cycle means that the converter is active for a longer duration, which allows for an increase in the output voltage.

Subsequently, the boost converter's output voltage is given by:

$$V_{out} = \frac{D}{1 - D}V_{in} \tag{9}$$

By analogy to Equation 9, the output current is expressed by the following relationship:

$$I_{out} = \frac{D}{1 - D}I_L \tag{10}$$

From Equations 9, 10 it is clear that the choice of the duty cycle D has a direct impact on the operation of the PVS through power optimization. Indeed, by adjusting D, the system can adapt to variations in sunlight and temperature, thus enabling optimal MPPT. Moreover, it is important to maintain a certain balance between power and efficiency. A duty cycle that is too high can lead to overheating losses and a reduction in converter efficiency, while a duty cycle that is too low may not allow reaching the desired output voltage V_{out}.

3.3 Output power of the boost converter

To find an expression for the output power P_{out} in terms of the duty cycle D and the input power P_{in}, we can proceed as follows:

$$P_{out} = V_{out}\, I_{out} \tag{11}$$

with P_{out} is the output power (W). By using Equations 9–11, we obtain:

$$P_{out} = \frac{D^2}{(1 - D)^2}V_{in}\, I_L \tag{12}$$

Since $I_{in} = I_L$, we can express the output power of the converter given by Equation 12 in conventional form in terms of the new duty cycle, described by the expression

$$P_{out} = D_P P_{in} \tag{13}$$

with D_P is the duty cycle corresponding to the output power of the converter, which can be written in the following form:

$$D_P = \frac{D^2}{(1 - D)^2} \tag{14}$$

Equations 13, 14 highlights the importance of choosing D_p to maximize the output power of a boost converter. Indeed, this relationship indicates that P_{out} is directly proportional to P_{in}. By maximizing D within safe limits, the system can extract the maximum available power from the photovoltaic panel.

4 The RVO technique

The integration of the RVO algorithm into the calculation of the duty cycle D optimizes the operation of the PVS. Therefore, it is essential to understand how to determine the reference voltage V_{ref}, which will subsequently be compared to V_{out}. Initially, the power-voltage characteristic is established based on the system's state of charge and variations in sunlight, as shown in Figure 1. By connecting all the maximum power points corresponding to the maximum voltage points of each curve, we obtain an inverse characteristic $V_{max} = f(P_{max})$. This characteristic describes the optimal operation for the MPP, which corresponds to the optimal reference voltage. Subsequently, the duty cycle D can be continuously recalculated to adapt to changes in V_{out} and V_{ref}, ensuring that the converter always operates at its maximum efficiency and maximizes power extraction, while highlighting the importance of dynamic voltage management in the PVS.

To make this technique more effective, the goal will be to maintain V_{in} at an optimal level to maximize the power extracted from the photovoltaic panel. To achieve this, we propose that the expression for the reference voltage V_{ref} is given by:

$$V_{ref} = k \times V_{in} \tag{15}$$

In Equation 15, k is a coefficient determined adaptively that adjusts the reference voltage based on the system's characteristics and sunlight conditions. To ensure that the voltage V_{ref} is as effective as possible, it is necessary to guarantee that k is optimal. To achieve this, we propose the algorithm for the implementation of RVO in the context of controlling the duty cycle D and optimizing k, given by the following Algorithm 1:

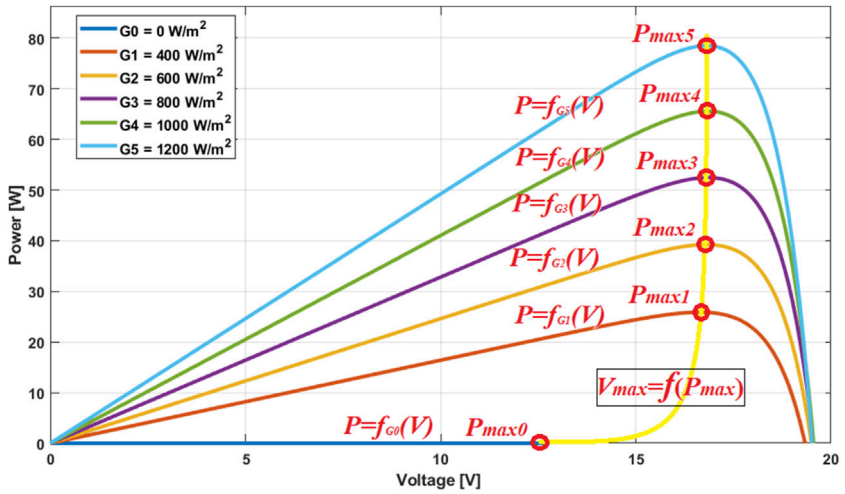

FIGURE 1
Power-voltage characteristic: Extraction of maximum power points.

```
BEGIN
  // Initialize parameters
  INITIALIZE Vref, k0, Pin, Pout
  SET alpha// Learning rate for gradient descent
  // Main loop
  WHILE (termination condition not met) DO
    // Measure Vin
    MEASURE Vin
    // Calculate Vref
    Vref = k * Vin
    // Calculate D
    D = Vout/ (Vout + Vin)
    // Evaluate output power
    Pout_new = D * Pin
    // Optimize k
    k_gradient = CALCULATE_gradient(Pout_new, k)
    // Calculate the derivative of Pout with respect to k
    k = k + alpha * k_gradient// Adjust k
    // Evaluate performance
    IF (Pout_new > Pout) THEN
      Pout = Pout_new// Keep the new Pout value
    ELSE
      k = k - alpha * k_gradient// Adjust k in the
    opposite direction
    END IF
  END WHILE
END
```

Algorithm 1. Adaptive RVO algorithm

5 Objectives of APISMC control

It should be noted that if the duty cycle is too large, i.e., very close to the value 1, it allows extracting the maximum power from the photovoltaic module but can cause overheating losses. On the other hand, if the duty cycle is very small, i.e., very close to the value 0, it does not allow reaching the desired output voltage V_{out}. This requires finding a balance between power and efficiency by adjusting the duty cycle. To this end, the objectives of the proposed APISMC control are such that:

The adaptive SMC aims to maintain the performance of the boost converter in the face of unexpected variations in system parameters, such as load changes or input voltage V_{in} fluctuations. This ensures stable regulation even under non-ideal conditions. Additionally, the use of an adaptive sliding surface improves the dynamic stability of the system. This means that the system can react quickly to changes in state and maintain the output voltage V_{out} at the reference value V_{ref} without undesirable oscillations, by appropriately adjusting the duty cycle D.

The APISMC allows quick and effective reaching of the MPPT by adjusting the duty cycle in real-time, according to changes in irradiance G G and temperature T. This control law is designed to maintain the system trajectory on the desired sliding surface chosen as a linear combination of state variable errors, typically the inductor current I_L and the output voltage V_{out}. Furthermore, the suitable choice of the sliding surface gains K_i will be made adaptively, allowing an optimization of the dynamic performance regulation of the system, such as response speed and stability.

Since variations in V_{in} can affect the output voltage V_{out} and disturbances can cause variations in the inductor current I_L, influencing the system stability, a disturbance-insensitive control like SMC is imperative to maintain the performance of the boost converter. For this, the dynamic adjustment of D allows compensating for disturbances and maintaining the output voltage V_{out} at the desired value V_{ref}, even in the presence of variations in V_{in} or load changes.

In summary, the objectives of the APISMC technique are as follows:

- Balance power and efficiency: Avoid overheating losses while ensuring the desired output voltage is achieved.
- Adapt to unexpected variations: Maintain performance in the face of changes in system parameters such as load variations or input voltage fluctuations.

- Improve dynamic stability: Ensure a rapid system response to state changes and maintain the output voltage at the desired reference value without undesirable oscillations.
- Rapidly achieve MPP: Adjust the duty cycle in real-time based on variations in irradiance and temperature to quickly reach the maximum power point.
- Ensure disturbance insensitivity: Maintain the performance of the boost converter even in the presence of disturbances and variations in input voltage or load.

6 Synthesis of the APISMC control

The design of the sliding surface ensures that the system remains stable during operation. By defining a specific trajectory for the system's state variables, it helps maintain the desired performance even under varying conditions. Additionally, it allows the control system to be robust against external disturbances such as changes in solar irradiance or temperature. This robustness is crucial for maintaining optimal performance in real-world scenarios.

The sliding surface S is defined by the following equation:

$$S = K_1\left(V_{ref} - V_{in}\right) + K_2\left(I_{ref} - I_L\right) \tag{16}$$

with and are weighting coefficients. The parameters K_1 and K_2 are weighting coefficients that determine the relative importance of the voltage error and current error in the sliding surface. One side, a higher value of K_1 means that the voltage error will have a greater impact on the sliding surface, leading to faster convergence of the actual voltage to the desired voltage. On the other side, a higher value of K_2 means that the current error will have a greater impact on the sliding surface, leading to faster convergence of the actual current to the desired current. Then, the parameters k1 and k2 are used to tune the performance of the APISMC control by adjusting the relative importance of the voltage and current errors in determining the sliding surface.

The sliding surface consists of the error between the desired and actual values of the voltage V_{in} and current I_L, it is used to validate the performance of the APISMC control. Regarding the boost converter, effective management of the system's trajectory on the sliding surface generates an optimal activation time that facilitates rapid responses to changes in environmental conditions, allowing for quick tracking of the maximum power point (MPP).

To introduce the PI part into the control, we modify the definition of I_{ref} so that it is calculated from the power error, which allows the system to be adaptive. The new expression for I_{ref} will be:

$$I_{ref} = I_{ref,0} + K_p\left(P_{ref} - P_{out}\right) + K_i \int \left(P_{ref} - P_{out}\right)dt \tag{17}$$

where $I_{ref,0}$ is the initial value of I_{ref} and P_{ref} is the desired output power.

The parameters K_i and K_p are used to implement the PI control for the system and used to tune the performance of the PI control by adjusting the relative importance of the current and accumulated errors in determining the control action. K_p is the proportional gain, which determines the response of the control system to the current error between the desired and actual output power. A higher value of K_p means that the controller will respond more aggressively to changes in the error. K_i is the integral gain, which determines the response of the control system to the accumulated error over time. A higher value of K_i means that the controller will be more persistent in reducing the error, even if it is small.

The sliding surface is designed by integrating the PI part into the surface given by Equations 16-17, we then obtain:

$$S = K_1\left(V_{ref} - V_{in}\right) + K_2\left(I_{ref,0} + K_p\left(P_{ref} - P_{out}\right) + K_i \int \left(P_{ref} - P_{out}\right)dt - I_L\right) \tag{18}$$

or alternatively

$$S = K_1\left(V_{ref} - V_{in}\right) + K_2\left(I_{ref,0} + K_p\epsilon_P + K_i \int \epsilon_P dt - I_L\right) \tag{19}$$

then

$$\epsilon_P = P_{ref} - P_{out} \tag{20}$$

To satisfy Equations 18–20 and to make the system adaptive, the gains K_1 , K_2 , K_p and K_i must be dynamically adjusted based on the system's performance. In our case, we will use optimization algorithms to adjust these gains, particularly the gradient descent algorithm; the various gains are given by:

$$\begin{cases} K_1 = K_1 - \alpha_1 \dfrac{\partial S}{\partial K_1} \\ K_2 = K_2 - \alpha_2 \dfrac{\partial S}{\partial K_2} \\ K_p = K_{\mathrm{p}} - \alpha_{\mathrm{p}} \dfrac{\partial S}{\partial K_{\mathrm{p}}} \\ K_i = K_i - \alpha_i \dfrac{\partial S}{\partial K_i} \end{cases}$$

where α_1, α_2, α_{p}, and α_{i} are positive learning rates. $\frac{\partial S}{\partial K_1}$, $\frac{\partial S}{\partial K_2}$, $\frac{\partial S}{\partial K_p}$ and $\frac{\partial S}{\partial K_i}$ are the partial derivatives of the sliding surface S with respect to each gain, and they will be calculated analytically. Once the surface S is designed, the adjustment of the duty cycle D is determined from its nominal value $D_0 = \frac{V_{out}}{V_{out}+V_{in}}$, its expression is provided by:

$$D = D_0 + K_s S \tag{21}$$

where K_s is a control gain to adjust the duty cycle based on the sliding surface. In the given context, K_s is defined as a control gain used to adjust the duty cycle D based on the sliding surface S. It plays a crucial role in tuning the response of the control system, allowing for modifications to the duty cycle to achieve the desired output performance. Specifically, K_s influences how much the duty cycle is adjusted in response to the state of the system as indicated by the sliding surface, helping to ensure a fast and robust response.

By using Equations 16, 21 we combine the two parts, the adaptive expression for D and incorporating both proportional and integral controls to ensure a fast and robust response of the system, can be formulated as follows:

$$D = D_0 + K_s\left(K_1\left(V_{ref} - V_{in}\right) + K_2\left(I_{ref} - I_L\right)\right) \tag{22}$$

The control gain K_s can be determined adaptively using the gradient descent method, defining the Cost Function as follows:

$$J(K_s) = \frac{1}{2}S^2 \tag{23}$$

The calculation of the derivative of the cost function with respect to K_s is given by:

$$\frac{\partial J}{\partial K_s} = S\frac{\partial S}{\partial K_s} \tag{24}$$

and the update of K_s is given by:

$$K_s = K_s - \alpha\frac{\partial J}{\partial K_s} \tag{25}$$

Using Equations 22–25, the expression for the control of the APISMC control system can be formulated by combining the contributions from the PI part and the SMC part, as follows:

$$D_{PI-SMC} = D_{PI} + D_{SMC} \tag{26}$$

The continuous component of the control is given by the PI control, as follows:

$$D_{PI} = K_p\left(P_{ref} - P_{out}\right) + K_i\int\left(P_{ref} - P_{out}\right)dt \tag{27}$$

The discontinuous component is given by:

$$D_{SMC} = K_sS \tag{28}$$

Thus, the final expression of the adaptive APISMC control to generate the duty cycle D for the boost converter is given by:

$$\begin{aligned} D = D_0 &+ K_p\left(P_{ref} - P_{out}\right) + K_i\int\left(P_{ref} - P_{out}\right) \\ &+ K_s\left(K_1\left(V_{ref} - V_{in}\right) + K_2\left(I_{ref} - I_L\right)\right) \end{aligned} \tag{29}$$

The switch activation duration t_{on} is related to the duty cycle D by the following relationship:

$$t_{on} = D\cdot T \tag{30}$$

where T is the total period of the cycle, which is the inverse of the switching frequency, given by:

$$T = \frac{1}{f} \tag{31}$$

Overall, this activation duration can be expressed in terms of the control as follows:

$$t_{on} = \frac{D_0 + K_p\left(P_{ref} - P_{out}\right) + K_i\int\left(P_{ref} - P_{out}\right) + K_s\left(K_1\left(V_{ref} - V_{in}\right) + K_2\left(I_{ref} - I_L\right)\right)}{f} \tag{32}$$

All the analytical relationships presented earlier for developing the sliding surface, the APISMC control given by Equations 26–29, and the switch activation duration given by Equations 30–32 are illustrated by the explanatory diagram in Figure 2. It is a diagram linking the different components of the PVS and the boost converter with the adaptive APISMC control, which is provided below.

To demonstrate the stability of the system using the candidate Lyapunov function, we will start from the inequalities and make simplifications through approximation. We will establish the conditions on the parameters that ensure the derivative of the Lyapunov function is negative.

We define the candidate Lyapunov function as follows:

$$V = \frac{1}{2}S^2 \tag{33}$$

where the sliding surface S is given by Equation 19. Then, $\dot{V}$ is obtained as:

$$\dot{V} = S\dot{S} \tag{34}$$

Calculating the derivative of the surface S:

$$\dot{S} = K_1\dot{V}_{ref} - K_1\dot{V}_{in} + K_2\left(K_p\dot{\epsilon}_P + K_i\epsilon_P + K_i\int\dot{\epsilon}_Pdt - \dot{I}_L\right) \tag{35}$$

For the system to be stable, we must have:

$$\dot{V} = S\dot{S} < 0 \tag{36}$$

using Equations 33–36, this implies that:

$$\begin{cases} S > 0 \\ \dot{S} < 0 \end{cases} \tag{37}$$

Considering the condition of Equation 37, we assume that the errors $|V_{ref} - V_{in}|$ and $|I_{ref} - I_L|$ are small, which allows us to write:

$$|S| \approx K_1\left|V_{ref} - V_{in}\right| + K_2\left|I_{ref,0} + K_p\epsilon_P + K_i\int\epsilon_Pdt - I_L\right| \tag{38}$$

Using absolute values, we can write:

$$|S| \le K_1\left|V_{ref} - V_{in}\right| + K_2\left(\left|I_{ref,0}\right| + K_p|\epsilon_P| + K_i\left|\int\epsilon_Pdt\right| - |I_L|\right) \tag{39}$$

Therefore, to ensure that $\dot{V} < 0$, we must have:

$$S\left(K_1\dot{V}_{ref} - K_1\dot{V}_{in} + K_2\left(K_p\dot{\epsilon}_P + K_i\epsilon_P + K_i\int\dot{\epsilon}_Pdt - \dot{I}_L\right)\right) < 0 \tag{40}$$

We generally consider that the derivatives $\dot{V}_{ref}$, $\dot{V}_{in}$, $\dot{\epsilon}_P$ and $\dot{I}_L$ are small, and we can further simplify them as follows:

$$\dot{S} = K_2\left(K_p\dot{\epsilon}_P + K_i\epsilon_P - \dot{I}_L\right) < 0 \tag{41}$$

For $\dot{S} < 0$, the gains must be sufficiently large. On one hand, this ensures that the current error and the voltage error are corrected quickly, and on the other hand, it guarantees a rapid response to power variations.

Considering Equations 37–41, in summary, if the gains K_1 , K_2 , K_p and K_i are sufficiently large, then it is possible to ensure that $\dot{V} < 0$ for positive values of S. This provides evidence that the system is stable, as the Lyapunov function decreases over time, implying that the states converge to equilibrium.

7 Numerical simulation

In this section, we will present the simulations conducted to validate the proposed control synthesis, namely, the APISMC control in the Matlab environment. These simulations aim to demonstrate the effectiveness and robustness of the APISMC in the context of MPPT for a photovoltaic system. By comparing the results obtained with those from conventional control methods, we will be able to evaluate the performance of the APISMC

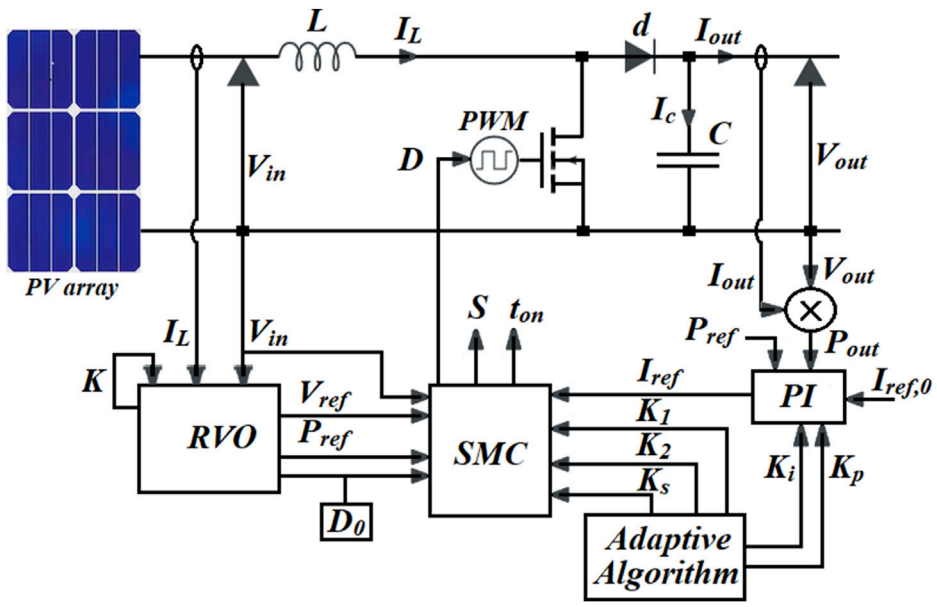

FIGURE 2
Diagram of the different components of the PVS system with the APISMC.

TABLE 1 The values of the photovoltaic system parameters.

Designation	Value
Nominal short-circuit current ($I_{sc,n}$)	$8,21\ A$
Short-circuit current temperature coefficient ($\mu_{I_{sc}}$)	$0,0032\ A/°C$
Nominal open-circuit voltage ($V_{oc,n}$)	$32,9\ V$
Open-circuit voltage temperature coefficient ($\mu_{V_{oc,n}}$)	$-0,1230\ V/°C$
Nominal current (I_n)	$7,61\ A$
Nominal voltage (V_n)	$26,3\ V$
Number of cells in series (N_s)	54
Diode ideality factor (a)	1,5

TABLE 2 The values of the boost converter parameters.

Designation	Value
Inductance of the inductor (L)	$2,2\ mH$
Capacitance of the capacitor (C)	$47\ \mu F$
Load resistance (R)	$100\ \Omega$

control in terms of stability, response speed, and ability to adapt to variations in environmental conditions.

We use a PV array containing 54 cells that are connected in series. The PV system delivers its power in parallel to the DC/DC boost converter. The parameters, including information on the electrical characteristics of the photovoltaic system under varying irradiation conditions, are provided below in Table 1.

The parameters, including information on the electrical characteristics of the boost converter under varying irradiation conditions, are provided below in Table 2.

The adaptive algorithms allow to obtain each time the values of the gains (K_1, K_2, K_s, K_i, K_p and k) for the control of the photovoltaic system.

For the case of the conventional SMC control, the parameters are manually adjusted to obtain the best responses, these parameters are given by:

$$K_1 = 78$$
$$K_2 = 37$$

Les valeurs du courant de référence et de duty cycle initiales sont données par:

$$I_{ref,0} = 15\ A$$

and

$$D_0 = 0.01$$

The simulations conducted have generated various figures illustrating the performance of the proposed APISMC control for the photovoltaic system and the boost converter. Figure 3 presents the solar irradiation profile used as input to the system, reflecting the variations in solar irradiation over time. Figures 4, 5 show the current and voltage control signals generated by the APISMC, respectively, highlighting its ability to dynamically adapt to changes in environmental conditions. Figure 6 compares the sliding surfaces obtained with the APISMC and the conventional SMC control, demonstrating the improvement brought by the integration of adaptive algorithms and the PI controller. Figures 7–9 present the responses of current, voltage, and power under the proposed APISMC control, comparing them to the performance of conventional SMC and PO techniques.

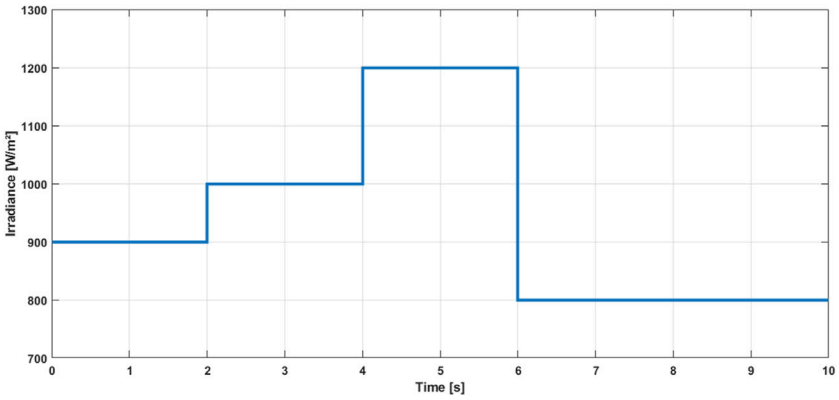

FIGURE 3
Sunlight profile defined by the received irradiation.

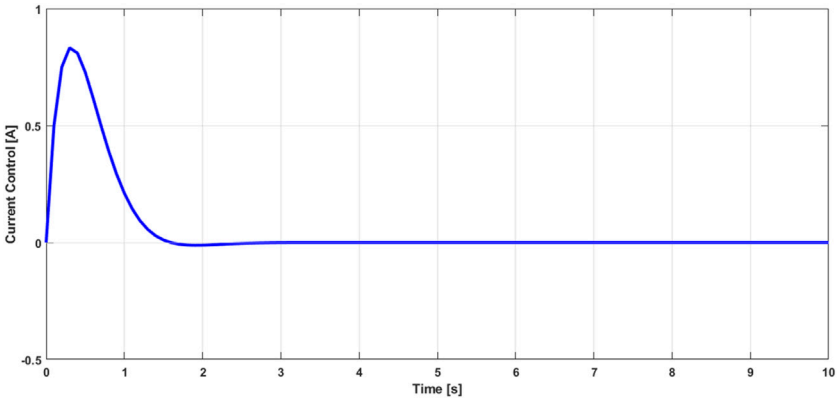

FIGURE 4
Current control signal generated by proposed scheme.

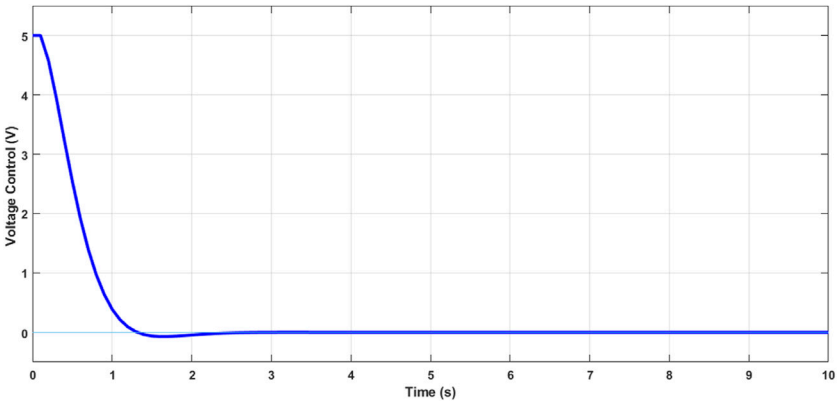

FIGURE 5
Voltage control signal generated by proposed scheme.

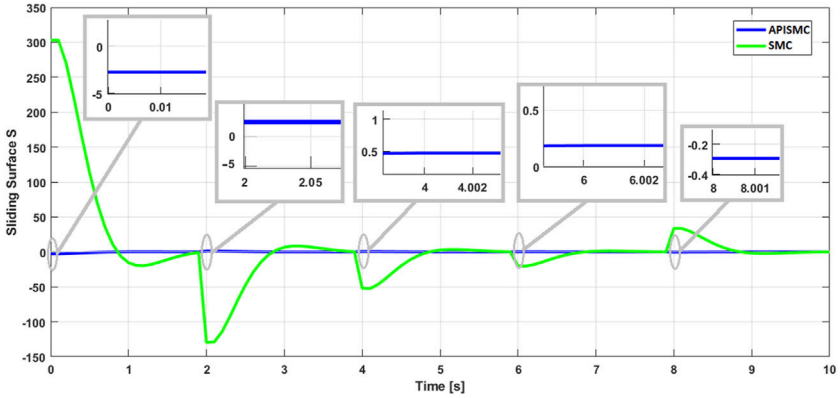

FIGURE 6
Sliding surface in both cases: conventional SMC and proposed PISMC.

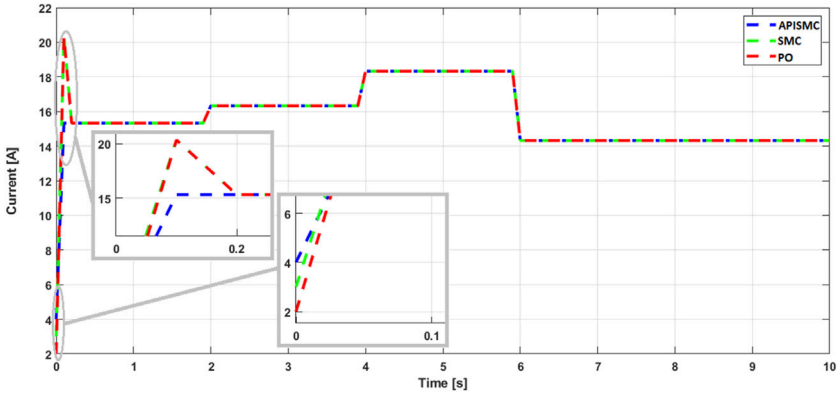

FIGURE 7
Current response by proposed APISMC and compared to SMC and PO.

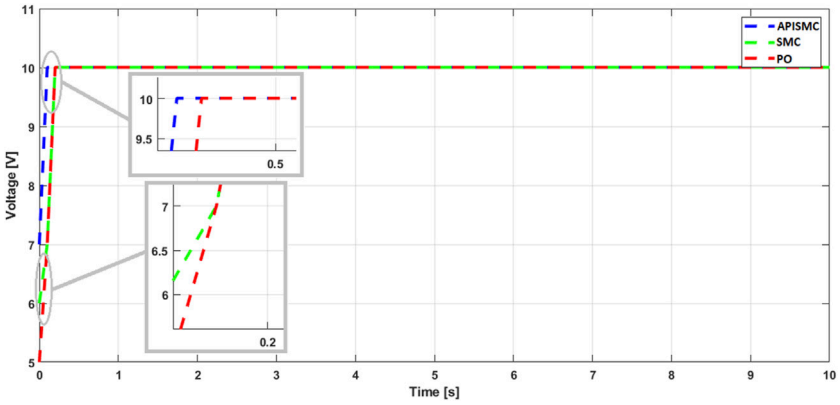

FIGURE 8
Voltage response by proposed APISMC and compared to SMC and PO.

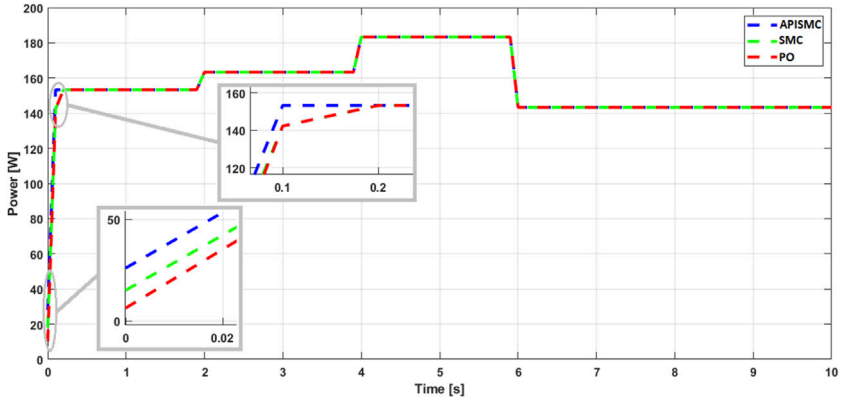

FIGURE 9
Power response by proposed APISMC and compared to SMC and PO.

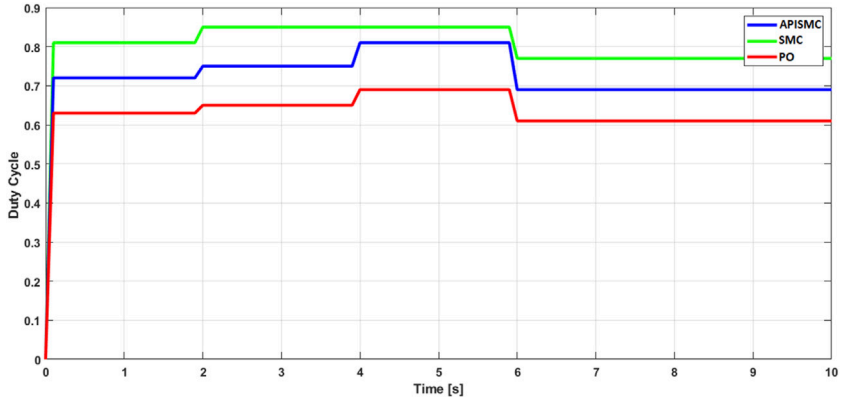

FIGURE 10
Duty cycle by proposed APISMC and compared to SMC and PO.

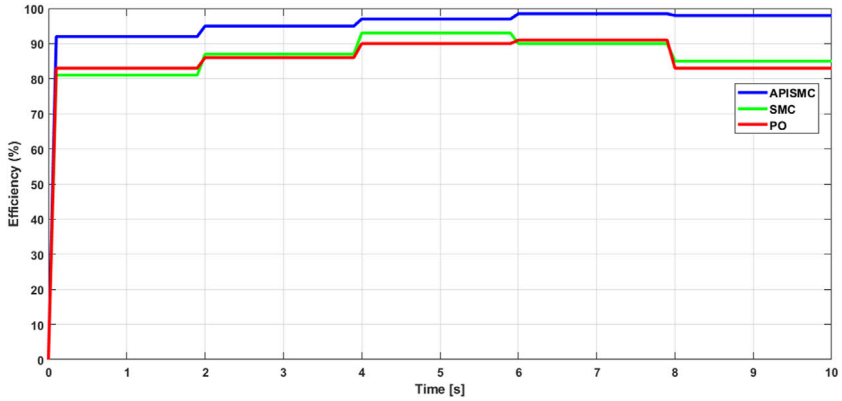

FIGURE 11
Efficiency of the different controls with temperature variation.

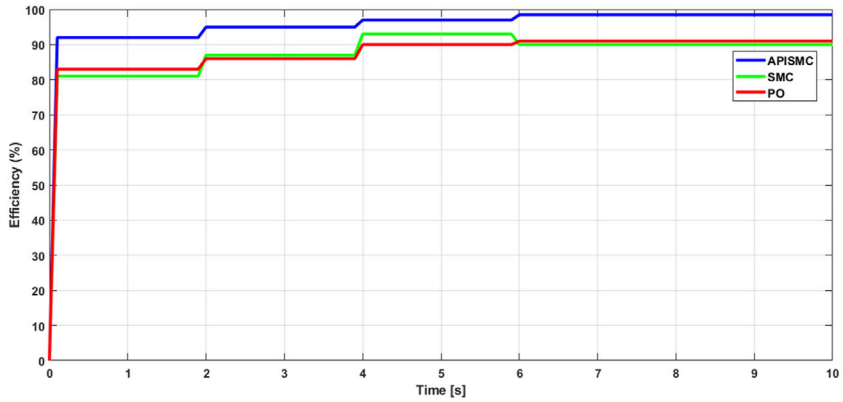

FIGURE 12
Efficiency of the different controls with irradiance variation.

Figure 10 illustrates the variation of the duty cycle D of the boost converter under different controllers: APISMC, SMC, and PO, emphasizing the optimization achieved by the APISMC to maximize the output power of the photovoltaic system. Finally, Figures 11, 12 demonstrate the impact of varying temperature and irradiance on the efficiency of different control strategies over time.

Figure 3 shows the variation of the solar irradiation received over time. The irradiation follows a distribution characterized by the successive values of $900\,W/m^2$, $1000\,W/m^2$, $1200\,W/m^2$, and $800\,W/m^2$. This variation in sunlight allows for the simulation of realistic conditions and the evaluation of the adaptive sliding mode control proposed by APISMC to quickly adapt to changes in irradiation to maintain the MPPT of the photovoltaic system.

There are minor fluctuations at the start of the signals shown in Figures 4, 5, but they quickly fade away after 2 *seconds*. The control input exhibits a very smooth signal without showing any chattering phenomena. The responses are provided for a solar irradiation of $900\,W/m^2$, and these signals repeat in the same manner for each variation in irradiation

Figure 6 presents the curve of the sliding surface S, whose evolution illustrates the variation of the signal representing the error of the current I_L and the voltage V_{in} relative to their optimal reference values I_{ref} and V_{ref}. By comparing the signals, it is clear that the sliding surface with the proposed APISMC control exhibits a very small norm on the order of −3, compared to the conventional SMC control, which has an amplitude of 300. Furthermore, the stability of the system is guaranteed despite variations in irradiation. Indeed, convergence is verified in both cases, which is typical of SMC in general. However, the response of the APISMC is very rapid, on the order of approximately 0.01 *seconds*, compared to that of the SMC, which spans the entire duration of the irradiation.

Overall, Figure 6 clearly demonstrates the effectiveness of the proposed control compared to SMC in mitigating the discrepancies between the system's behavior and the optimal reference values. This highlights the effectiveness of the adaptive part of the control in optimizing the calculated values of I_{ref} and V_{ref}, as well as all the gains K_1, K_2, K_s, K_i, K_p and k.

The simulations in Figures 7–9 present the variations of current, voltage, and typical power. Stability is achieved, with different convergence characteristics among the controls. The simulations of current, voltage, and power show that the proposed control exhibits a minimal response time of 0.1 *seconds*, as well as a settling time of less than 0.1 *seconds* compared to other controls, such as SMC and PO control. The proposed APISMC-controlled system has been thoroughly verified to ensure its dynamic behavior delivers both high accuracy and speed.

These results highlight the effectiveness of the APISMC control in regulating the performance of the photovoltaic system. The rapid response of the control allows for effective adaptation to variations in sunlight conditions, thus ensuring optimal power extraction. In comparison, other control methods show longer settling times, which can affect their ability to react quickly to fluctuations in irradiation. Additionally, the APISMC control does not exhibit overshoot, unlike other controls that may reach an overshoot of 14%.

The validity of the APISMC compared to other control methods, namely, SMC and PO, is clearly demonstrated in the management of the duty cycle D of the boost converter. In Figure 10, the simulations show that the APISMC allows for a more precise and responsive adjustment of the duty cycle, resulting in effective optimization of the output power. Indeed, in the case of SMC control, an insensitivity is identified regarding the variation of irradiation between $900\,W/m^2$, $1000\,W/m^2$ and $1200\,W/m^2$. The SMC control does not react and maintains the same value of D, which is 0.85 for these irradiation values. The PO control maintains a similar response to that of the APISMC but with lower amplitudes.

The simulations presented above in Figures 11, 12 were conducted by varying environmental conditions, specifically temperature and irradiance, to evaluate the performance of different MPPT control strategies. The results demonstrate that the APISMC consistently outperforms both SMC and PO in terms of efficiency. This superiority can be attributed to the adaptive and

flexible nature of the APISMC parameters, allowing it to adjust in real-time to environmental variations. Consequently, APISMC is capable of maintaining an optimal operating point for the boost converter, regardless of temperature or irradiance, resulting in higher energy yields.

Simulations conducted with temperatures ranging from 15°C to 45°C and irradiance levels between 800 W/m^2 and 1200 W/m^2 revealed that APISMC achieved an average of 5% higher efficiency compared to SMC and PO. This improvement is due to APISMC's ability to continuously adjust its parameters based on rapid irradiance fluctuations, enabling it to more accurately track the maximum power point. Additionally, APISMC's robustness to disturbances, such as load variations, contributes to maintaining high efficiency under real-world conditions.

8 Results and discussion

The study has conclusively demonstrated the superiority of the APISMC controller over conventional SMC and PO control methods in the context of PV systems. Based on the simulations from the previous section, APISMC has excelled in several areas:

- Stability and responsiveness: The control signals generated by APISMC are remarkably smooth, indicating high system stability. Additionally, APISMC's response time is significantly faster, enabling it to react quickly to variations in environmental conditions.
- Power optimization: By dynamically adjusting the duty cycle of the boost converter, APISMC effectively maximizes the output power of the PV system. This capability is essential for making the most of available solar energy.
- Adaptability: Thanks to its adaptive nature, APISMC can quickly adapt to changes in solar irradiance, which is particularly important in environments with variable weather conditions.
- Robustness: APISMC has demonstrated high robustness to disturbances, maintaining stable control even under challenging conditions. These superior performances can be attributed to the integration of adaptive algorithms and a PI controller within APISMC. These elements enable the controller to adapt in real-time to system variations and continuously optimize its performance. In comparison, conventional SMC and PO methods struggle to adapt quickly to environmental changes and may exhibit oscillations or slower response times. The efficiency results obtained in the simulations confirm these observations, showing that APISMC consistently outperforms other control methods. The use of APISMC in PV systems can lead to a significant increase in energy efficiency and better utilization of solar energy. Furthermore, the robustness and adaptability of APISMC make it a promising solution for applications in diverse and demanding environments. Overall, the proposed control exhibits a minimal response time, allowing for rapid adjustment of the duty cycle in response to variations in irradiance. This not only guarantees maximum power extraction but also ensures better system stability. In comparison, other control methods, while effective in certain conditions, exhibit longer stabilization times and reduced responsiveness, which can lead to performance losses in dynamic environments. Thus, APISMC proves to be a superior approach for duty cycle control, ensuring optimal converter management and maximizing PV system efficiency.

However, the APISMC control method has several limitations. First, its design and implementation can be quite complex, given the number of parameters used, especially with adaptive dynamics. Furthermore, the control gains must also be carefully tuned to ensure optimal performance, leading to a tuning process that can be time-consuming. Additionally, the computational cost associated with the calculations necessary for real-time adaptation can pose challenges in applications where processing resources are limited. These limitations emphasize the importance of thorough evaluation and testing in real conditions to ensure the method's effectiveness in practical applications.

9 Conclusion

This article presents an in-depth study on the application of Proportional-Integral Sliding Mode Adaptive Control (APISMC) aimed at maximizing the output power of a photovoltaic system (PVS) through a boost converter. The main results of the simulations demonstrate the effectiveness of the proposed APISMC method compared to conventional Maximum Power Point Tracking (MPPT) techniques. The APISMC method significantly outperforms traditional MPPT algorithms such as Sliding Mode Control (SMC) and Perturb and Observe (PO) control, particularly under rapidly changing environmental conditions, proving its performance. In terms of robustness against variations, the integration of a Reference Voltage Optimizer (RVO) enables the APISMC to dynamically adapt to fluctuations in solar irradiation and temperature, thereby ensuring optimal power extraction in variable conditions. The simulations confirm that the proposed control method maintains system stability and responds quickly to changes in irradiation, effectively tracking the maximum output power while minimizing oscillations. The combination of adaptive control strategies with SMC leads to improved robustness and performance, making APISMC an optimal approach.

Overall, the results indicate that the APISMC method not only enhances the efficiency of photovoltaic systems but also provides a reliable solution for maximizing energy production in the face of environmental uncertainties. However, it is important to note certain drawbacks associated with the APISMC method. Notably, the complexity of implementing APISMC requires intricate modeling and precise parameter calibration, which can make its implementation more challenging compared to simpler methods. Another weakness is that the adaptive algorithm may demand greater computational resources, which may not be feasible in low-cost or low-power systems. To address this, several perspectives can be considered to improve the reliability and practical application of this control method. For this purpose, it would be interesting to integrate the proposed control with artificial intelligence techniques, as the use

of machine learning and neural networks could further enhance the adaptability of the control.

Data availability statement

The original contributions presented in the study are included in the article/supplementary material, further inquiries can be directed to the corresponding authors.

Author contributions

BT: Conceptualization, Formal Analysis, Methodology, Validation, Visualization, Writing–original draft, Writing–review and editing. AA: Conceptualization, Formal Analysis, Investigation, Methodology, Supervision, Writing–original draft, Writing–review and editing. AS: Conceptualization, Formal Analysis, Methodology, Resources, Visualization, Writing–original draft, Writing–review and editing. SA: Formal Analysis, Investigation, Methodology, Resources, Validation, Writing–original draft, Writing–review and editing. IH: Data curation, Formal Analysis, Investigation, Methodology, Resources, Writing–review and editing, Funding acquisition. IK: Data curation, Formal Analysis, Resources, Validation, Writing–review and editing, Investigation, MA: Data curation, Formal Analysis, Resources, Software, Validation, Writing–review and editing.

Funding

The author(s) declare that financial support was received for the research, authorship, and/or publication of this article. This research was funded by Norwegian University of Science and Technology, Norway. This research was also supported by the Automated Systems and Soft Computing Lab (ASSCL), Prince Sultan University, Riyadh, Saudi Arabia.

Acknowledgments

The authors would like to thank the Norwegian University of Science and Technology, Norway for paying the Article Processing Charges (APC) for this publication. The authors specially acknowledge the Automated Systems and Soft Computing Lab (ASSCL) at Prince Sultan University, Riyadh, Saudi Arabia. In addition, the authors wish to acknowledge the editor and reviewers for their insightful comments, which have improved the quality of this publication. The authors would like to thank Prince Sultan University, Riyadh, Saudi Arabia, for support with the article processing charges.

Conflict of interest

The authors declare that the research was conducted in the absence of any commercial or financial relationships that could be construed as a potential conflict of interest.

Publisher's note

References

Abdelmalek, S., Azar, A. T., and Dib, D. (2018). A novel actuator fault-tolerant control strategy of DFIG-based wind turbines using Takagi-Sugeno Multiple models. *Int. J. Control, Autom. Syst.* 16 (3), 1415–1424. doi:10.1007/s12555-017-0320-y

Ahmed, E. M., Norouzi, H., Alkhalaf, S., Ali, Z. M., Dadfar, S., and Furukawa, N. (2022). Enhancement of MPPT controller in PV-BES system using incremental conductance along with hybrid crow-pattern search approach based ANFIS under different environmental conditions. *Sustain. energy Technol. assessments* 50, 101812. doi:10.1016/j.seta.2021.101812

Ali, A. I. M., and Mohamed, H. R. A. (2022). Improved P&O MPPT algorithm with efficient open-circuit voltage estimation for two-stage grid-integrated PV system under realistic solar radiation. *Int. J. Electr. Power & Energy Syst.* 137, 107805. doi:10.1016/j.ijepes.2021.107805

Aljafari, B., Balachandran, P. K., Samithas, D., and Thanikanti, S. B. (2023). Solar photovoltaic converter controller using opposition-based reinforcement learning with butterfly optimization algorithm under partial shading conditions. *Environ. Sci. Pollut. Res.* 30 (28), 72617–72640. doi:10.1007/s11356-023-27261-1

Alnami, H., Hakmi, S. H., Abdelwahab, S. A. M., Abdellatif, W. S., Hegazy, H. Y., Mohamed, W. I., et al. (2024). Enhanced adaptive dynamic surface sliding mode control for optimal performance of grid-connected photovoltaic systems. *Sustainability* 16 (13), 5590. doi:10.3390/su16135590

Atia, M., Bouarroudj, N., Ahriche, A., Djari, A., and Houam, Y. (2022). Maximum power harvesting from a PV system using an improved two-stage MPPT scheme based on incremental conductance algorithm and integral controller. *Int. J. Model. Identif. Control* 40 (2), 176–191. doi:10.1504/IJMIC.2022.124722

Azar, A. T., and Serrano, F. E. (2015). "Stabilization and control of mechanical systems with backlash," in *Handbook of research on advanced intelligent control engineering and automation, advances in computational intelligence and robotics (ACIR) book series, USA* (USA: IGI Global), 1–60.

Bhat, S., Nagaraja, H. N., and Thakur, P. (2020). DSP based proportional integral sliding mode controller with fast exponential reaching law for photo-voltaic system. *Int. J. Adv. Res. Eng. Technol. (IJARET)* 11 (5), 597–605. doi:10.34218/IJARET.11.5.2020.062

Cano, A., Arévalo, P., and Jurado, F. (2024). Neural network predictive control in renewable systems (HKT-PV) for delivered power smoothing. *J. Energy Storage* 87, 111332. doi:10.1016/j.est.2024.111332

Chaibi, Y., Salhi, M., and El-Jouni, A. (2019). Sliding mode controllers for standalone PV systems: modeling and approach of control. *Int. J. Photoenergy* 2019 (1), 1–12. doi:10.1155/2019/5092078

Chandrashekar, B., Pradeep, J., Sivasubramanian, M., Khandan, K. L., and Dhanraj, J. A. (2024) "A fuzzy logic controller for a photovoltaic system relying on a closed-loop DC-DC converter," in Ninth international conference on science Technology engineering and mathematics (ICONSTEM), Chennai, India, 04–05 April, 2024. doi:10.1109/ICONSTEM60960.2024.10568741

Chang, Y., Yu, W., Luo, M., Zhou, F., Huang, W., and Zhai, G. (2024). Anti-interference control method of buck–boost converter based on high-order nonlinear disturbance observer. *Electronics* 13 (7), 1318. doi:10.3390/electronics13071318

Chellakhi, A., El Beid, S., Abouelmahjoub, Y., and Doubabi, H. (2024). An enhanced incremental conductance MPPT approach for PV power optimization: a simulation and experimental study. *Arabian J. Sci. Eng.* 49, 16045–16064. doi:10.1007/s13369-024-08804-1

Chinnappan, R., Logamani, P., and Ramasubbu, R. (2019). Fixed frequency integral sliding-mode current-controlled MPPT boost converter for two-stage PV generation system. *IET Circuits, Devices & Syst.* 13 (6), 793–805. doi:10.1049/iet-cds.2018.5221

Corrêa, H. P., and Vieira, F. H. T. (2023). Hybrid sensor-aided direct duty cycle control approach for maximum power point tracking in two-stage photovoltaic systems. *Int. J. Electr. Power & Energy Syst.* 145, 108690. doi:10.1016/j.ijepes.2022.108690

Derbeli, M., Napole, C., and Barambones, O. (2023). A fuzzy logic control for maximum power point tracking algorithm validated in a commercial PV system. *Energies* 16 (2), 748. doi:10.3390/en16020748

El Fadili, A., Giri, F., and El Magri, A. (2014). Reference voltage optimizer for maximum power point tracking in triphase grid-connected photovoltaic systems. *Int. J. Electr. Power & Energy Syst.* 60, 293–301. doi:10.1016/j.ijepes.2014.03.029

El Ouardi, H., El Gadari, A., Mokhlis, M., Ounejjar, Y., Bejjit, L., and Al-Haddad, K. (2023). A Novel MPPT technique based on combination between the incremental conductance and hysteresis control applied in a standalone PV system. *Eng* 4 (1), 964–976. doi:10.3390/eng4010057

Ezhilan, T., Govindharaj, A., Ambikapathy, A., Prajapati, B. M., Kumar, M., Singh, A. V., et al. (2022). "Adaptive sliding mode fuzzy logic controller for PV battery system," in 2022 2nd international conference on advance computing and innovative technologies in engineering (ICACITE), Greater Noida, India, 28–29 April, 2022. doi:10.1109/ICACITE53722.2022.9823722

Gomathi, S., Mayurappriyan, P. S., and BabyPriya, B. (2024). Performance improvement of grid-tied PV system with boost and quadratic boost converters using innovatory hybridized HPO-PO MPPT. *Electr. Power Components Syst.*, 1–13. doi:10.1080/15325008.2024.2318399

Gundecha, A. D., Gohokar, V. V., Mahapatro, K. A., and Suryawanshi, P. V. (2016). "Control of DC–DC converter in presence of uncertain dynamics,". *Intelligent systems technologies and applications. Advances in intelligent systems and computing*. Editors S. Berretti, S. Thampi, and P. Srivastava (Cham: Springer), 384, 315–326. doi:10.1007/978-3-319-23036-8_27

Henao-Bravo, E. E., Ramos-Paja, C. A., and Saavedra-Montes, A. J. (2022). Adaptive control of photovoltaic systems based on dual active bridge converters. *Computation* 10 (6), 89. doi:10.3390/computation10060089

Hussain, K., Kaliappan, S., Saini, P., Kumar, S. N., and Dhanraj, J. A. (2024). "PV generation monitoring using calculated power flow from μPMUS," in 2024 international conference on optimization computing and wireless communication (ICOCWC), Debre Tabor, Ethiopia, 29–30 January, 2024. doi:10.1109/ICOCWC60930.2024.10470487

Kumar, V., and Bindal, R. K. (2022). MPPT technique used with perturb and observe to enhance the efficiency of a photovoltaic system. *Mater. Today Proc.* 69, A6–A11. doi:10.1016/j.matpr.2023.01.002

Li, N. Z., Jiang, Y. X., and Wei, X. J. (2024). Model-free adaptive chaos control for the boost converter. *Meas. Control* 57 (5), 519–529. doi:10.1177/00202940231194117

Maguluri, L. P., Farook, S., Saravanan, R., Dixit, A., Aishwarya, K. P., and Dhanraj, J. (2023). "An appraisal in to the effects of partial shading on an urban photovoltaic system using the internet of things," in 2023 international conference on advances in computing, communication and applied informatics (ACCAI), doi:10.1109/ACCAI58221.2023.10201066

Mazumdar, D., Sain, C., Biswas, P. K., Sanjeevikumar, P., and Khan, B. (2024). Overview of solar photovoltaic MPPT methods: a state of the art on conventional and artificial intelligence control techniques. *Int. Trans. Electr. Energy Syst.* 2024 (1), 1–24. doi:10.1155/2024/8363342

Muktiadji, R. F., Ramli, M. A., Bouchekara, H. R., Milyani, A. H., Rawa, M., Seedahmed, M. M., et al. (2022). Control of boost converter using observer-based backstepping sliding mode control for DC microgrid. *Front. Energy Res.* 10, 828978. doi:10.3389/fenrg.2022.828978

Oh, J., So, D., Jo, J., Kang, N., Hwang, E., and Moon, J. (2024). Two-Stage neural network optimization for robust solar photovoltaic forecasting. *Electronics* 13 (9), 1659. doi:10.3390/electronics13091659

Oliver, J. S., David, P. W., Balachandran, P. K., and Mihet-Popa, L. (2022). Analysis of grid-interactive PV-fed BLDC pump using optimized MPPT in DC–DC converters. *Sustainability* 14 (12), 7205. doi:10.3390/su14127205

Ouaret, A., Lehouche, H., Oubelaid, A., Yadav, A., Mendil, B., and Zaitsev, I. (2023). Maximum power extraction in photovoltaic systems using high-performance adaptive control approach. *Int. J. Photoenergy*, 2023(1), 1. 16. doi:10.1155/2023/6506144

Poongavanam, P., Chand, A. A., Tai, V. B., Gupta, Y. M., Kuppusamy, M., Dhanraj, J. A., et al. (2023). Annual thermal management of the photovoltaic module to enhance electrical power and efficiency using heat batteries. *Energies* 16 (10), 4049. doi:10.3390/en16104049

Radhakrishnan, R. K. G., Marimuthu, U., Balachandran, P. K., Shukry, A. M. M., and Senjyu, T. (2022). An intensified marine predator algorithm (MPA) for designing a solar-powered BLDC motor used in EV systems. *Sustainability* 14 (21), 14120. doi:10.3390/su142114120

Rahme, S. Y., Islam, S., Amrr, S. M., Iqbal, A., Khan, I., and Marzband, M. (2023). Adaptive sliding mode control for instability compensation in DC microgrids due to EV charging infrastructure. *Sustain. Energy, Grids Netw.* 35, 101119. doi:10.1016/j.segan.2023.101119

Remoaldo, D., and Jesus, I. (2021). Analysis of a traditional and a fuzzy logic enhanced perturb and observe algorithm for the MPPT of a photovoltaic system. *Algorithms* 14 (1), 24. doi:10.3390/a14010024

Ruz-Hernandez, J. A., Garcia-Hernandez, R., Ruz Canul, M. A., Guerra, J. F., Rullan-Lara, J. L., and Vior-Franco, J. R. (2024). Neural sliding mode control of a buck-boost converter applied to a regenerative braking system for electric vehicles. *World Electr. Veh. J.* 15 (2), 48. doi:10.3390/wevj15020048

Sahoo, S., Amirthalakshmi, T. M., Ramesh, S., Ramkumar, G., Arockia Dhanraj, J., Ranjith, A., et al. (2022). Artificial deep neural network in hybrid PV system for controlling the power management. *Int. J. Photoenergy* 2022 (1), 1–12. doi:10.1155/2022/9353470

Said Adouairi, M., Bossoufi, B., Motahhir, S., and Saady, I. (2023). Application of fuzzy sliding mode control on a single-stage grid-connected PV system based on the voltage-oriented control strategy. *Results Eng.* 17, 100822. doi:10.1016/j.rineng.2022.100822

Samadhiya, A., and Namrata, K. (2021). Probabilistic screening and behavior of solar cells under Gaussian parametric uncertainty using polynomial chaos representation model. *Complex & Intelligent Syst.* 8 (2), 989–1004. doi:10.1007/s40747-021-00566-9

Samadhiya, A., Namrata, K., and Gupta, D. (2021). Uncertainty quantification in deterministic parameterization of single diode model of a silicon solar cell. *Optim. Eng.* 22 (4), 2429–2456. doi:10.1007/s11081-021-09679-z

Saxena, H., Singh, A., and Rai, J. N. (2021). RNN based control algorithm for power quality improvement in PV integrated distribution system. *Electr. Power Components Syst.* 49 (9-10), 849–859. doi:10.1080/15325008.2022.2049646

Singh, S., Azar, A. T., Ouannas, A., Zhu, Q., Zhang, W., and Na, J. (2017). "Sliding mode control technique for multi-switching synchronization of chaotic systems," in 2017 9th international conference on modelling, identification and control (ICMIC), Kunming, China, 10–12 July, 2017, 880–885.

Stitou, M., El Fadili, A., Chaoui, F. Z., and Giri, F. (2022). Adaptive output-feedback control design for maximum power point tracking of uncertain photovoltaic systems. *IFAC J. Syst. Control* 21, 100205. doi:10.1016/j.ifacsc.2022.100205

Swarnkar, P., Gawre, S. K., and Akodiya, G. (2022). "Comparative Analysis of conventional and sliding mode control techniques for DC-DC boost converter for PV system under transient conditions,". *Recent advances in power electronics and drives. Lecture notes in electrical engineering*. Editors S. Kumar, B. Singh, and A. K. Singh (Singapore: Springer), 852, 587–600. doi:10.1007/978-981-16-9239-0_45

Tian, Z., Lyu, Z., Yuan, J., and Wang, C. (2019). UDE-based sliding mode control of DC–DC power converters with uncertainties. *Control Eng. Pract.* 83, 116–128. doi:10.1016/j.conengprac.2018.10.019

Vaidyanathan, S., and Azar, A. T. (2016). A novel 4-D four-wing chaotic system with four quadratic nonlinearities and its synchronization via adaptive control method. Advances in chaos theory and intelligent control. *Stud. Fuzziness Soft Comput.* 337, 203–224. doi:10.1007/978-3-319-30340-6_9

Vankadara, S. K., Chatterjee, S., and Balachandran, P. K. (2023). "Applications of metaheuristic algorithms for MPPT under partial shaded condition in PV system," in 2023 4th international conference for emerging Technology (INCET), Belgaum, India, 26–28 May, 2023 (IEEE), 1–5.

Vankadara, S. K., Chatterjee, S., Balachandran, P. K., and Mihet-Popa, L. (2022). Marine predator algorithm (MPA)-based MPPT technique for solar PV systems under partial shading conditions. *Energies* 15 (17), 6172. doi:10.3390/en15176172

Velmurugan, K., Elavarasan, R. M., De, P. V., Karthikeyan, V., Korukonda, T. B., Dhanraj, J. A., et al. (2022). A review of heat batteries based PV module cooling—case studies on performance enhancement of large-scale solar PV system. *Sustainability* 14 (4), 1963. doi:10.3390/su14041963

Wang, J., Gao, Y., Zhao, Y., Feng, Z., and Liu, J. (2023). A comparative study of FNN-based dynamic sliding mode control for DC-DC converters. *Int. J. Circuit Theory Appl.* 51 (2), 579–593. doi:10.1002/cta.3446

Youssef, A. R., Hefny, M. M., and Ali, A. I. M. (2023). Investigation of single and multiple MPPT structures of solar PV-system under partial shading conditions considering direct duty-cycle controller. *Sci. Rep.* 13 (1), 19051. doi:10.1038/s41598-023-46165-1

10.3389/fenrg.2024.1485470

Nomenclatures

I_{ph}	Photocurrent (A)
I_0	Saturation current (A)
V_{pv}	Voltage of the PV module (V)
R_s	Series resistance (Ω)
a	Quality factor of the diode
N_s	Number of PV cells in series
V_{th}	Thermal voltage (V)
$I_{sc,n}$	Nominal short-circuit current (A)
k_i	Temperature coefficient of the short-circuit current (%/°C)
T	Cell temperature (°C)
T_n	Nominal temperature (°C)
G	Incident irradiance (W/m^2)
G_n	Nominal irradiance (W/m^2)
C	Capacitance of the boost converter circuit capacitor in (F)
L	Inductance of the coil in (H)